Journal of Hazardous Materials 509 (2026) 142030

Contents lists available at ScienceDirect

Journal of Hazardous Materials

journal homepage: www.elsevier.com/locate/jhazmat

Phragmites australis and *Scirpus holoschoenus* for metal(loid)s polluted groundwater remediation: a wetland mesocosm study with different exposure regimes

Aqib Hassan Ali Khan [a,*,1], Alberto Soto-Cañas [a,1], Carlos Rad [b], Andrea Martin-Pablo [a], Blanca Velasco-Arroyo [c], Dalia de la Fuente-Vivas [a], Laura Gómez-Cuadrado [a], Gonzalo Salazar-Mardones [c], Herwig De Wilde [d], Alfredo Pérez-de-Mora [e], Rocío Barros [a,*]

[a] *International Research Center in Critical Raw Materials for Advanced Industrial Technologies (ICCRAM), University of Burgos, Centro de I+D+I, Plaza Misael Bañuelos s/n, Burgos 09001, Spain*
[b] *Research Group in Composting (UBUCOMP), University of Burgos, Faculty of Sciences, Plaza Misael Bañuelos s/n, Burgos 09001, Spain*
[c] *Department of Biotechnology and Food Science, University of Burgos, Plaza Misael Bañuelos, s/n, Burgos 09001, Spain*
[d] *TAUW België nv, Dept. of Soil and Groundwater, Waaslandlaan 8A3, Lokeren 9160, Belgium*
[e] *TAUW GmbH, Dept. of Soil and Groundwater, Louise-Ulrich-Straße 14, Munich 80636, Germany*

HIGHLIGHTS

- Metal(loid)s polluted groundwater phytoremediation in different regimes was studied.
- *P. australis* and *S. holoschoenus* performed phytostabilization of metal(loid)s.
- Mesocosms neutralized water pH (3.7–7.6), promoting to metal immobilization.
- Treated water restored the HepG2 cell viability, hence reducing health risk.
- Both plants showed higher tolerance and biomass in chronic exposure.

GRAPHICAL ABSTRACT

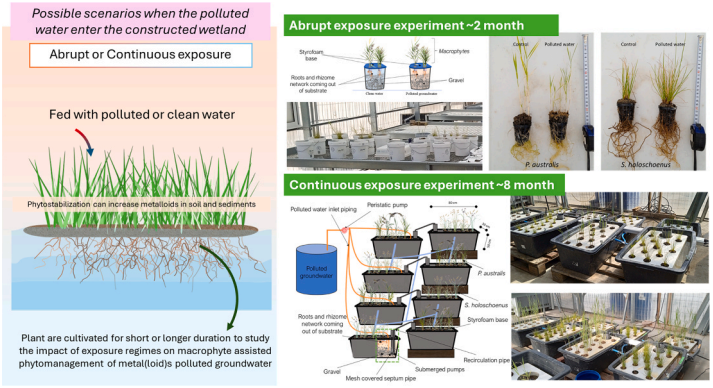

ARTICLE INFO

Keywords:
Macrophytes
Groundwater
Metal(loid)s
Wetlands
Toxicity

ABSTRACT

Mitigation of pollutants is crucial for long-term sustainable management of groundwater and freshwater systems and ecosystem health. However, the potential of nature-based attenuation strategies, such as phytoremediation, in the presence of multi-element contamination and under changing exposure conditions, remains largely unexplored. This study aimed to comprehensively assess the potential of *Phragmites australis* and *Scirpus holoschoenus* for metal(loid) remediation in contaminated groundwater. The investigation involved both medium (4 L) static and large dynamic (65 L) mesocosms to simulate different exposure conditions, including abrupt

* Corresponding authors.
E-mail addresses: ahkhan@ubu.com (A.H.A. Khan), rbarros@ubu.es (R. Barros).
[1] Both authors contributed equally

https://doi.org/10.1016/j.jhazmat.2026.142030
Received 10 December 2025; Received in revised form 17 March 2026; Accepted 9 April 2026
Available online 12 April 2026

(acute), and continuous (progressive and chronic), with a particular focus on reducing overall metal(loid) toxicity. Dynamic mesocosm results demonstrated that both macrophytes corrected water pH from 3.7 to 7.6, and significantly reduced Ni, Fe, and Cu, which initially exceeded the Flemish regulatory limits by up to 3182-fold. Additionally, *P. australis* exhibited superior bioenergy potential, with higher heating values (HHV) reaching up to 17.15 MJ kg^{-1}. Metal uptake followed a clear phytostabilization trend for Al, Cu, Fe, Ni, and Zn. Most notably, macrophytes assisted phytoremediation restored the HepG2 cell viability from 0% to over 75%, indicating an effective neutralization of polluted groundwater toxicity. In conclusion, this study demonstrated the potential of phytoremediation using *P. australis* and *S. holoschoenus* as sustainable strategy for contaminated water treatment, providing simultaneous benefits of metalloids removal, toxicity reduction, and the valorization of biomass for bioenergy applications.

1. Introduction

The discharge of metal(loid)s into a wetland ecosystem due to natural or anthropogenic sources can be detrimental to aquatic life and human health, as these systems are particularly vulnerable to such fluctuations [1,2]. Natural factors include strata geology, water-rock interactions, and weathering of deposits, while the anthropogenic activity is primarily linked with ill-managed industrial activities and disposals. In particular, the interface where contaminated groundwater discharges into wetland systems creates a complex biogeochemical zone where metal(loid)s mobility is highly sensitive to fluctuating the hydrogeological conditions [3,4]. For instance, the groundwater quality in former industrial areas is often very poor due to historical waste disposal. Seasonal aquifer fluctuations can create alternating static and dynamic hydraulic conditions. However, most phytoremediation studies are conducted in uniform flow setups, failing to capture the complexity of real-world groundwater-wetland interfaces [5,6]. If not properly managed, these legacy inorganic pollutants will be reintroduced into terrestrial and aquatic environments, necessitating proper disposal and or treatment mechanisms [7]. Adverse consequences include impaired growth and impaired reproductive cycles of flora and fauna and a decline in ecosystem services, like nutrient cycling and pollutant removal [8,9].

Macrophytes contribute to the natural attenuation of pollutants via processes such as phytoextraction, phytostabilisation and rhizofiltration [10,11]. These processes involve the uptake, immobilization and precipitation of metals and metalloids by plant roots and associated microorganisms [12]. Hence, to mitigate metal(loid)s impacts, metal(loid)s-tolerant macrophytes, such as *Phragmites australis* and *Scirpus holoschoenus,* can be utilized [13,14]. While these macrophytes have shown capacity for water remediation, their comparative efficacy under varying hydraulic stress remains poorly understood [15,16]. The temporal nature of pollution can alter the long-term stabilization of metals and metalloids in aquatic systems [17]. Polechońska and Klink [18] suggested that the biological (plant type, genetic profile, growth and development stage) and nonbiological factors (water pH, salinity, redox potential, exposure time, metal speciation) influence the metal availability and toxicity. Similarly, Serafini et al. [19] proposed that the wetland sediments act as binding sites and natural sink for metals and metalloids in the different geochemical phases reflecting their mobility, bioavailability, and their potential risk to the biota. Therefore, a holistic assessment should integrate metal(loid) uptake, and speciation in the sediments, under varying exposure regimes [19,20].

Macrophytes play a crucial role in maintaining the health of wetlands, even in the presence of metal and metalloid contamination [18]. Strategically introducing these plants in contaminated wetlands can reduce the bioavailability of metal(loid)s and mitigate their toxic effects on other organisms. It can be hypothesized that groundwater phytoremediation using different types of macrophyte, in different growing conditions, can result in changes in the phytoremediation efficiency. However, high removal percentage does not always correlate to the reduction in biological toxicity of the treated effluent, and it necessitates a combined chemical analysis and bio-toxicological assessment [21,22]. This will answer a critical question of how different exposure patterns (i.e. acute, progressive or continual exposure) affect plant resilience and contaminant partitioning, and whether the treated water meets safety levels for the residual toxicity.

In the present study macrophyte based phytoremediation was employed to treat polluted groundwater, to reduce the environmental impact and meet the Flemish sanitation standards for water discharge (in μg L^{-1} Ni 40, Cu 100, Fe 200, Zn 500, As 20, Cd 5 and Pb 20). Therefore, the main aim of this work is to evaluate the phytoremediation capacity of *P. australis* and *S. holoschoenus* for removing metal(loid)s from groundwater under both static and dynamic (recirculating) conditions. Additionally, the study evaluates the impact of different exposure regimes (progressive, acute, and chronic) on plant growth, metal compartmentalization, and toxicity reduction following phytoremediation of polluted groundwater.

2. Materials and methodology

2.1. Chemicals and reagents

Analytical and reagent grade solvents, solutions, and salts (including acetone ≥99.5%, hydrogen peroxide 33%, hydrochloric acid 37%, nitric acid 65%, tris-(hydroxymethyl)-aminomethane 99.8%, maleic acid 99%, citric acid 99.5%, boric acid 99.5%, sodium hydroxide 97%, fluorogenic 4-methylumbelliferone ≥ 98%, amino-4-methylcoumarin - ≥ 98%, hydroxylamine hydrochloride, sodium acetate 99.9%, magnesium chloride 98%, ammonium acetate 99%, sodium pyruvate 99%, sodium bicarbonate 99%, and Fetal Bovine Serum) were acquired from Merck Life Science S.L.U. (Madrid, Spain) or VWR International (Barcelona, Spain). All solutions were prepared in ultrapure water (specific resistance of 18.2 MΩ cm) generated by an ELGA PURELAB Classic CLX DIM2 system (ELGA LabWater, High Wycombe, UK).

2.2. Plants, growth conditions, and polluted groundwater characterization

P. australis and *S. holoschoenus* seedlings were obtained from Viveros La Dehesa, Valdeobispo, Spain. Seedlings were maintained on a photoperiod of 16:8 h light:darkness at 25:16 °C for day:night, at the plant growth facility of the Universidad de Burgos, Spain. Groundwater with elevated metal(loid) concentrations (notably Pb, Cu, Zn, As, and Ni) was obtained from an industrial site in Flanders (Belgium) previously described [23]. The polluted groundwater (PW) was characterized having an acidic pH of 3.7 and a moderately high EC of 5.3 dS m^{-1}. Metal(loid) concentrations (expressed in mg L^{-1}) Al 305.1, As 0.3, Cd 2, Cr 0.1, Cu 163, Fe 382, Ni 127, Pb 0.3, and 72 for Zn. The concentrations of all elements except for Fe (no regulatory limit) were significantly above the Flemish BSN regulatory values (remediation required). Consequently, the metal and metalloid concentrations exceeded the maximum permissible limits of Flemish sanitation standards by the following folds: Ni (3182), Fe (1910), Cu (1632), Cd (441), Zn (143), As (16), and Pb (16).

2.3. Experimental conditions and exposure regimes

For the evaluation of the macrophyte tolerance capacity to polluted groundwater, experiments were performed in 2 different setups, each targeting a different exposure route: i) abrupt (subsection 2.3.1) and ii) continuous (subsection 2.3.2). The images of the acute exposure regime experiment and the macrophyte floating system are shown in Figures S1 and S2 of the supplementary material, respectively.

2.3.1. Abrupt exposure regime

For the abrupt exposure (Abr) experiment, uniform-sized plants were directly exposed to either polluted groundwater or non-polluted (tap) water as control using 4 L bucket batches. For each treatment, two plantlets of uniform size (growing on peat growth substrate - GS) were introduced onto a circular extruded polystyrene holding piece. This piece had holes to allow plastic baskets for root development and water sampling/monitoring within the microcosm floating system. Briefly, the 4 L buckets used were made of polypropylene, with height of 19.7 cm, while top and bottom radius of 8.7 and 8.6 cm, respectively (max capacity 4.6 L). Each microcosm was filled with 2 L water rinsed medium–fine gravel (4.75 – 10 mm, with porosity of 38.2%), while the remaining volume (~2.76 L) was filled either with polluted or clean water (depending on the treatment). Plants were exposed to these conditions for 2 months. Throughout the exposure duration, water levels were maintained with tap water to compensate for any losses due to evapotranspiration. Subsequently, plants, growth substrate and sediments were harvested for analysis of physico-chemical and biological parameters. The analyses included pH, electrical conductivity (EC), and salinity (Sal) in water, metal(loid)s in water, growth substrate and plants, metal(loid) speciation and soil enzyme activities in growth substrate. Analytical methods are described in Sections 2.4–2.9.

2.3.2. Continuous exposure regime

The experiment was conducted in eight interconnected wetland mesocosms (black PVC plastic containers with W×L×H dimensions of 45 ×75 ×30 cm), each with a total volume of ~65-liter. There were 4 mesocosms per plant species (*P. australis* and *S. holoschoenus*). The containers were initially filled with fine-medium gravel (4.75 – 10 mm) to reach a total porosity of 38.2%, a specific yield of 34% and a specific retention of 4.2%. The void gravel spaces (~25 L per mesocosm) were filled with tap water. Equal sized young seedlings (3–4 weeks old) of *P. australis* and *S. holoschoenus,* (growing on peat GS) were planted on a floating Styrofoam sheet. On each floating sheet a total of 12 plants were placed in a similar way to 4 L mesocosm. Initially, plants were acclimatized in non-polluted water for 2 weeks.

After this acclimatization, the first phase of exposure initiated in which the plants were irrigated with polluted groundwater, at an HRT of 60 days, which was maintained using flow rates (Q) of ~2.90 L week^{-1} per mesocosm. The flow rates were maintained considering the specified HRT (t), gravel porosity Φ), system depth (y), and area (A) and were calculated using Eq. (1).

$$HRT = \frac{A \times y \times \Phi}{Q} \quad (1)$$

Based on the flow rates (~2.90 L) and concentration of metal(loid)s in polluted water (mg L^{-1}), used to irrigate in the wetland mesocosm, the loading rates of each metal(loid)s per mesocosm (mg week^{-1}) were calculated using Eq. (2).

$$L = Q \times C \quad (2)$$

Hence, the loading rate (mg week^{-1}) identified during polluted groundwater irrigation were as follow Fe 1107.8, Al 884.79, Cu 472.70, Ni 368.3, Zn 208.8, Cd 5.80, As 0.87, Pb 0.87, and Cr 0.29. As there were 8 interconnected mesocosms, that total pollutant loadings per week (mg week^{-1}) were as follow Fe 8862.4, Al 7078.32, Cu 3781.60, Ni 2946.40, Zn 1670.40, Cd 46.40, As 6.96, Pb 6.96, and Cr 2.32. A recirculation pump was used to feed the polluted groundwater in the wetland system, while inter-mesocosm was maintained by submerged pumps (Supplementary figure 2.a). During the first 4 months of exposure (first phase), the plants were irrigated only with the polluted water. During the first phase approximately 403 L of polluted groundwater were treated in the interconnected mesocosms. After this exposure, half of the plants were harvested (representatives of progressive exposure, Pro), and plant physiological parameters were determined.

The harvested plants were replaced by new seedlings of the same species of equal size (representatives of acute exposure, Acu). The other half of the plants (representatives of chronic exposure, Chr), that were initially included in the mesocosms, were left undisturbed to examine the changes in plant metal uptake for another 4 months (second phase). During this time the water level in the constructed wetland was maintained solely using tap water. After 4 months of the second phase, plants were harvested and growth substrate, water, and gravel were sampled. Physiological parameters, elemental composition and gross higher heating values were assessed in plants (Section 2.4). Physico-chemical parameters and metal(loid) concentrations were measured in water (Sections 2.5 and 2.6). The metal(loid) content was analysed in both dried plants and growth substrate (Section 2.7), while the gravel samples were also subjected to metal sequential extraction analysis (Section 2.8). The wetland water was sampled also at the end of the mesocosms experiment for ecotoxicological profiling (Section 2.9).

2.4. Plant characterization: biomass production, photosynthetic pigments, and higher heating values

Following harvest, fresh and dry biomass (roots and shoots) was quantified gravimetrically and reported as g ± g. The dry biomass was estimated by heating a sample at 60 °C until attaining constant weight [12]. With the help of fresh and dried biomass, the water content (g) was calculated using the following Eq. (3).

$$Water\ content = Fresh\ weight - Dried\ weight \quad (3)$$

Photosynthetic pigments were extracted from leaf samples in triplicate by homogenizing with 80% acetone and briefly centrifuging at 12,000 *g* [24]. The supernatant was analyzed for pigments (total chlorophyll, chlorophyll a, chlorophyll *b*, and carotenoids) using an UV-Vis spectrophotometer (Synergy HT BioTek, Vermont USA). Contents were calculated using Eqs. 4–7 and values expressed in mg g^{-1} fresh weight:

$$Chlorophyll\ A\ (Chla) = \frac{(12.25\ Abs_{663.2} - 2.79\ Abs_{646.8}) \times V}{1000 \times W} \quad (4)$$

$$Chlorophyll\ B\ (Chlb) = \frac{(21.50\ Abs_{646.8} - 5.10\ Abs_{663.2}) \times V}{1000 \times W} \quad (5)$$

$$Total\ Chlorophyll\ (TChl) = Chla + Chlb \quad (6)$$

$$Total\ Carotenoids\ (Car) = \frac{(1000\ Abs_{470} - 1.82\ Chla - 85.02\ Chlb) \times V}{198 \times 1000 \times W} \quad (7)$$

Where the calculation variables are $Abs_{663.2}$, $Abs_{646.8}$, and Abs_{470} (absorbance at 663.2, 646.8, and 470 nm), V (solution volume in μL), and W (fresh biomass weight in g).

For the estimation of the capacity of biomass to be used as a feedstock biofuel, gross higher heating values (HHVs) were calculated for different types of biomasses produced within progressive, acute, and chronic exposure [25]. The value of biomass HHVs was expressed as an MJ of energy per kg of dried biomass [26,27], and calculated using Eq. (8):

$$HHV = 0.3516C + 1.16225H - 0.1109O + 0.0628N + 0.10465S \quad (8)$$

For this purpose, the C, H, N, O, and S total contents were quantified in milled plant samples using an automated dry combustion Flash 2000 CHNS/O microanalyzer (Thermo Fisher Scientific, Milan, Italy), the system operated via automated dry combustion at 1100 °C. Alfalfa as a certified standard for calibration purposes (Ref. 502–273, LECO Corporation, St. Joseph, Michigan, USA).

2.5. Physical parameters of water

Water physico-chemical parameters (including pH, oxidation reduction potential – ORP, electrical conductance – EC, resistivity – Res, total dissolved solids – TDS, and salinity – Sal) were characterized using HI 98194 Multiparameter cell, Hanna Instruments, USA. Calibration of multimeter was performed using the company provided calibration standard solution of pH 4, 7, and 8. For the exposure experiments in 4 L buckets the analysis of physico-chemical parameters was performed on a weekly basis for 2 months, while for the wetland mesocosms the water was analysed twice monthly for 8 months.

2.6. Soil enzyme activities

Enzyme activities in growth substrate, including acid phosphatases (AcPA), β-glucosidase (bGA), N-acetyl-β-glucosaminidase (bNAG), and leucyl-aminopeptidase (LeuAMP), were measured using fluorogenic 4-methylumbelliferone (MUF) or amino-4-methylcoumarin (AMC)-substrates in 96-microtiter plates [28]. Frozen growth substrate samples (1 g) were suspended in 20 mL of sterilized and deionized water and subjected to pulsed sonication (40 W) for 2 min, for soil extract preparation. For each respective enzymatic assay, 50 μL of GS extract aliquot was mixed with 50 μL of 500 μM of Modified Universal Buffer (MUB), at a pH adjusted between 5–10, depending on the enzyme activity. Subsequently, the samples were incubated at 30 °C for 3 h. The reaction was terminated by addition of tris buffer (pH 12).

The samples were analysed on a fluorometric plate-reader (TECAN Group Ltd., Männedorf, Switzerland) at 360 and 450 nm. Fluorescence was converted into product amounts (MUB or AMC) using a calibration standard (0–1500 pmol) converted to product amounts (MUB/AMC) via calibration standards that accounted for quenching and expressed in soil enzyme activities nmol g^{-1} min^{-1}.

2.7. Sequential metal(loid)s extraction

The gravel samples were subjected to sequential fractionation for the determination of the exchangeable, carbonate, Fe and Mn oxide, organic matter, and residual fractions [29,30]. Dry samples (1.0 g) were sequentially extracted with i) 1 M $MgCl_2$ (pH 7) (exchangeable fraction), ii) 1 M NaOAc (pH 5) (carbonate bound), iii) 0.04 M hydroxylamine hydrochloride in 25% acetic acid (Fe- and Mn-oxides adsorbed – reducible), and iv) 0.02 M HNO_3 + 30% H_2O_2 (pH 2) and subsequently with 3.2 M ammonium acetate in 20% HNO_3 (organically bound – oxidizable). The solid residue was rinsed with DI water between extraction steps [29], and finally, metal(loid)s in residual form were assessed as in Section 2.8.

2.8. Metal(loid)s content in plant, soil, and water

The metal(loid) concentrations in water samples were analysed after centrifugation, filtration, and acidification using (1:9 v:v) concentrated HNO_3 to water sample [31]. For assessing metal(loid) concentrations in plant and GS samples, they were firstly dried at 60 °C until constant weight was reached, and subsequently subjected to acid digestion with 2 mL of 33% v/v H_2O_2 and 8 mL of 65% concentrated nitric acid using a microwave oven (ETHOS ONE, Millestone, USA), for 20 min at 190 °C [32,33]. For quality assurance rye grass-certified standard material (ERM-CD281), soil standard (BCR-483), and blanks were included in digestion batches. The final digested solutions were filtered using Scharlau CF/WASH110 filter paper (Ø 110 mm) and brought to a final volume of 50 mL with deionized water.

Finally, metal(loid) concentrations (mg kg^{-1}) in the extracts and water were measured via ICP–OES (SpectroGenesis or Arcos, AMETEC, Germany) and ICP-MS/MS (8900, Agilent, USA). The accuracy of instrumental measurements for plant samples ranged between highest recovery of 98.18 ± 1.87 for Zn, to lowest recovery of Ni 95.5 ± 4.78, corresponding to the standard certified reference material (SRM) ERM-CD281. While highest recovery of 97.28 ± 2.91 for Cu to lowest recovery of Cd 96.94 ± 3.18, corresponding to the SRM BCR-483.

2.9. HepG2 Dynamic Spheroid Formation and Viability Assessment

Advanced 3D cell culture methodology was employed using HepG2 spheroids as an *in vitro* liver model to assess the cytotoxicity of groundwater samples. The 3D format was selected due to its improved physiological relevance over traditional 2D cultures, allowing for a more representative evaluation of potential human health risks. Spheroids were generated according to the protocol described by Štampar et al., [34] and incubated for 3 days at 37 °C in a humidified atmosphere containing 5% CO_2. Following this initial incubation, spheroids were transferred to the CelVivo system (CelVivo ApS, Værløse, Denmark), a norm gravity, omnidirectional clinostat bioreactor [35,36], and cultured under dynamic conditions for an additional 17 days. After 20 days of culture, spheroids were harvested for viability assessment and a 24-hour acute exposure assay using groundwater samples from phytoremediation experiments. Prior to exposure, water samples were filtered through 0.2 μm PES membranes to remove potential microbial contaminants, preventing confounding effects due to microbial metabolism during assays and ensuring accurate downstream analyses.

Acute exposures were performed using 90% (v/v) water samples diluted in 10x Minimum Essential Medium (MEM) supplemented with 1% Fetal Bovine Serum (FBS), 1% sodium pyruvate, and 2% $NaHCO_3$. The 90% concentration was selected to simulate high exposure levels, allowing sensitive detection of cytotoxic responses to groundwater contaminants. Three water conditions were tested: (i) non-polluted water previously exposed to *P. australis* and *S. holoschoenus*, (ii) non-treated polluted water, and (iii) phytoremediated water collected at the final timepoint following plant exposure. Appropriate controls, including untreated spheroids and vehicle controls, were included to validate the specificity of the observed effects. Intracellular ATP levels were quantified for post-exposure to assess cytotoxicity. Total protein content was determined using the Bradford assay to normalize ATP levels to cellular biomass, following the protocols of Fey and Wrzesinski [35] and Wrzesinski et al. [36], respectively.

2.10. Statistical analysis

All analytical procedures were performed under strict quality control protocols. All samples were analyzed in triplicate (n = 3), and the standard deviation (SD) was maintained below 5%. Reagent blanks were processed alongside every batch of samples to monitor potential contamination. One-way ANOVA was performed to test significant differences between treatments using the software SPSS v.20. All the

analyses were performed in triplicate. In addition, Duncan's multiple range test was also performed ($p \leq 0.05$) to assess the differences between specific groups/parameters from each other in all data collected, except in the case of HepG2 spheroid viability where Dunnet multiple comparisons test was applied. The mean and the standard deviation were calculated using triplicates of biological data. To better identify the underlying patterns and relationships between the parameters studied and plant type, a multivariate principal component analysis (PCA) was performed also with the software SPSS v.20. Scatter plots were constructed using the loading values of the first 2 principal components (having eigen values greater than 1).

3. Results

3.1. Abrupt exposure experiment in 4 L batch mesocosms

3.1.1. Plant physiological parameters

The comparison of parameters studied for *P. australis* and *S. holoschoenus*, both cultivated in 4-L mesocosms and subjected to an Abr exposure, is presented in Table 1. In *P. australis* no significant changes were noted in plant biomass (fresh and dried) and heights for both roots and shoots, except in the case of change in root length, which was significantly higher for plants cultivated in polluted water (12.27 ± 1.87). In contrast, for *S. holoschoenus*, the fresh and dried weights for shoot biomass were found to be significantly different between plants cultivated with non-polluted control and polluted water. Fresh weight (5.18 ± 0.74), dried weight (1.54 ± 0.25), and plant water content (3.63 ± 0.50) of *S. holoschoenus* were 68, 69, and 67% higher in plants cultivated with polluted water than those of plants cultivated with non-polluted water. For the content of the chlorophyll pigments including Chl A, Chl B, Total Chl, and Carotenoids (Car), no significant differences were observed between non-polluted control and polluted water irrigation.

3.1.2. Studied properties of plant growth substrate and sediments

For enzyme activities no clear trend was observed in mesocosms with *P. australis* including an increase in AcPA (42.37 ± 4.36) and bNAG (55.21 ± 7.36), no change in bGA (6.56 ± 1.21), and decrease in LeuAMP (92.48 ± 17.5) when plants were exposed to polluted water. On the contrary, a significant decrease was observed for all enzyme activities in mesocosms with *S. holoschoenus* exposed to polluted water compared to non-polluted controls. The metal(loid) concentrations in the rhizospheric GS are shown in Table 1. For *P. australis* and *S. holoschoenus*, respectively, higher concentrations (mg kg^{-1}) of Cu (1990.81 ± 458.55 and 1238.57 ± 194.61), Fe (4357.59 ± 818.80 and 3380.26 ± 239.81), Ni (1230.40 ± 105.18 and 1383.95 ± 225.00), and Zn (528.29 ± 41.35 and 551.94 ± 111.19) were noted in mesocosms exposed to polluted water than non-polluted controls.

In addition, the metal(loid) fractionation in sediments is shown in Fig. 1. Polluted water cultivated treatments showed significantly higher variation in the metal(loid)s fractions compared to control. The speciation of metal(loid)s in GS varied between elements as well as between the non-polluted control and polluted treatments, except for chromium (Cr) and iron (Fe). The most relevant differences in speciation were

Table 1
Plant and soil characteristics following harvest for the 4 L mesocosm experiments.

Matrice and parameter*		*P. australis*		*S. holoschoenus*	
		Con[1]	Pol[1]	Con[1]	Pol[1]
Shoot (Stem + Leaves)	FW	1.08 ± 0.19 a	1.65 ± 0.41 a	3.08 ± 0.91 b*	5.18 ± 0.74 a*
	DW	0.70 ± 0.12 a	0.77 ± 0.16 a	0.91 ± 0.22 b*	1.54 ± 0.25 a*
	WC	0.38 ± 0.17 b	0.88 ± 0.26 a	2.17 ± 0.70 b	3.63 ± 0.50 a*
	IL	15.48 ± 3.73 a	16.10 ± 6.43 a	13.60 ± 3.52 a	16.35 ± 3.76 a
	FL	21.08 ± 4.59 a*	23.10 ± 6.24 a*	16.33 ± 5.13 a	18.23 ± 3.79 a
	CL	5.60 ± 2.45 a*	7.00 ± 1.31 a*	2.73 ± 2.20 a	1.88 ± 0.26 a
Root	FW	3.00 ± 0.61 a	3.46 ± 0.85 a	4.61 ± 1.87 a	4.19 ± 1.39 a
	DW	0.84 ± 0.02 a	0.68 ± 0.12 a	1.29 ± 0.26 a*	0.80 ± 0.19 a*
	WC	2.16 ± 0.63 a	2.78 ± 0.73 a	3.32 ± 2.03 a*	3.39 ± 1.20 a
	IL	21.13 ± 8.14 a*	13.48 ± 5.70 b*	8.90 ± 3.40 a	7.10 ± 2.42 b
	FL	27.82 ± 8.39 a	25.75 ± 6.56 a	25.92 ± 4.40 a	22.58 ± 1.45 a
	CL	6.69 ± 1.08 b	12.27 ± 1.87 a	17.02 ± 4.11 a*	15.49 ± 2.96 a*
Leaves	Chl A	0.43 ± 0.16 a	0.64 ± 0.13 a*	0.33 ± 0.06 a	0.43 ± 0.15 a
	Chl B	0.10 ± 0.04 a	0.15 ± 0.03 a	0.08 ± 0.01 a	0.11 ± 0.04 a
	Total Chl	0.53 ± 0.20 a	0.79 ± 0.16 a*	0.41 ± 0.07 a	0.54 ± 0.18 a
	Car	0.05 ± 0.02 a	0.08 ± 0.02 a	0.04 ± 0.01 a	0.05 ± 0.02 a
	Chl a/Chl b	4.44 ± 0.33 a	4.38 ± 0.06 a	4.14 ± 0.15 a	4.08 ± 0.21 a
	Total Chl/Car	9.77 ± 0.56 a	9.57 ± 0.02 a	10.15 ± 0.41 a	10.14 ± 0.49 a
Growth substrate	AcPA	27.87 ± 3.96 b*	42.37 ± 4.36 a*	16.15 ± 3.3 a	11.68 ± 2.89 b
	bGA	7.36 ± 1.06 a	6.56 ± 1.21 a	13.59 ± 1.97 a*	10.15 ± 3.24 b*
	bNAG	84.17 ± 21.31 a*	55.21 ± 7.36 a*	75.76 ± 5.9 a	32.46 ± 6.49 b
	LeuAMP	117.73 ± 20.45 a*	92.48 ± 17.51 b*	101.7 ± 9.89 a	47.02 ± 3.85 b
	Al	1049.57 ± 158.74 a	1025.87 ± 244.02 a	876.54 ± 37.37 a	946.79 ± 107.34 a
	As	1.58 ± 0.15 b	2.50 ± 0.28 a	1.50 ±.29 b	2.50 ± 0.14 a
	Cd	1.12 ± 0.29 b	8.71 ± 3.08 a	0.96 ± 0.25 b	8.12 ± 3.87 a
	Cr	2.36 ± 0.28 b	3.87 ± 0.63 a	1.95 ± 0.25 b	3.61 ± 0.52 a
	Cu	28.85 ± 2.75 b	1990.81 ± 458.55 a	31.3 ± 2.69 b	1238.57 ± 194.61 a
	Fe	1638.79 ± 337.55 b	4357.59 ± 818.8 a	1742.39 ± 34.9 b	3380.26 ± 239.81 a
	Ni	4.91 ± 1.13 b	1230.40 ± 105.18 a	3.24 ± 0.43 b	1383.95 ± 225.00 a
	Pb	0.83 ± 0.38 b	8.00 ± 0.96 a*	1.16 ± 0.90 b	5.83 ± 0.52 a
	Zn	33.81 ± 10.46 b	528.29 ± 41.35 a	15.13 ± 1.04 b	551.94 ± 111.19 a

* Parameters studied are abbreviated as FW = Fresh weight, DW = Dried weight, and WC = Water content in shoot, root, and soil (g), while IL = Initial length, FL= Final length, CL = Change in length noted for shoot and root (cm), AcPA = Acid phosphatase, bGA = β-glucosidase, bNAG = N-acetyl-glucosidase, and LeuAMP = leucyl- aminopeptidase for soil (nmol g^{-1} min^{-1}), and Chl A = Chlorophyll A, Chl B = Chlorophyll B, Total Chl = Total Chlorophyll, and Car = Catenoids (mg g^{-1} FW), while Chl A/Chl B and Total Chl/Car are the ratios for leaves. Metal and metalloid contents in soil are expressed in mg kg^{-1}. [1]Con = Control (tap water irrigated population), while Pol = Polluted water exposed population. Different letters between rows of the same species (a being significant higher followed by other alphabets), while * between same treatment displays significant statistical differences at $p < 0.05$.

reported for Cu and Ni, both present at very different concentrations in control and polluted GSs, as well as for As, present at similar concentrations in both treatments. Generally, the speciation of metal(loid)s in GS was similar for both plants and controls without plants exposed to the same type of water, suggesting that the presence of the plants had no significant effect.

3.1.3. Water physicochemical parameters

The distribution of the water parameters data is shown in box and whisker plots (prepared using measurements at weekly intervals for 2 months, n = 8) on Fig. 2. Significant differences were observed for pH, ORP, EC, TDS, and Sal between polluted and non-polluted controls, but also temporarily for the same treatment. In this manner, the pH of the

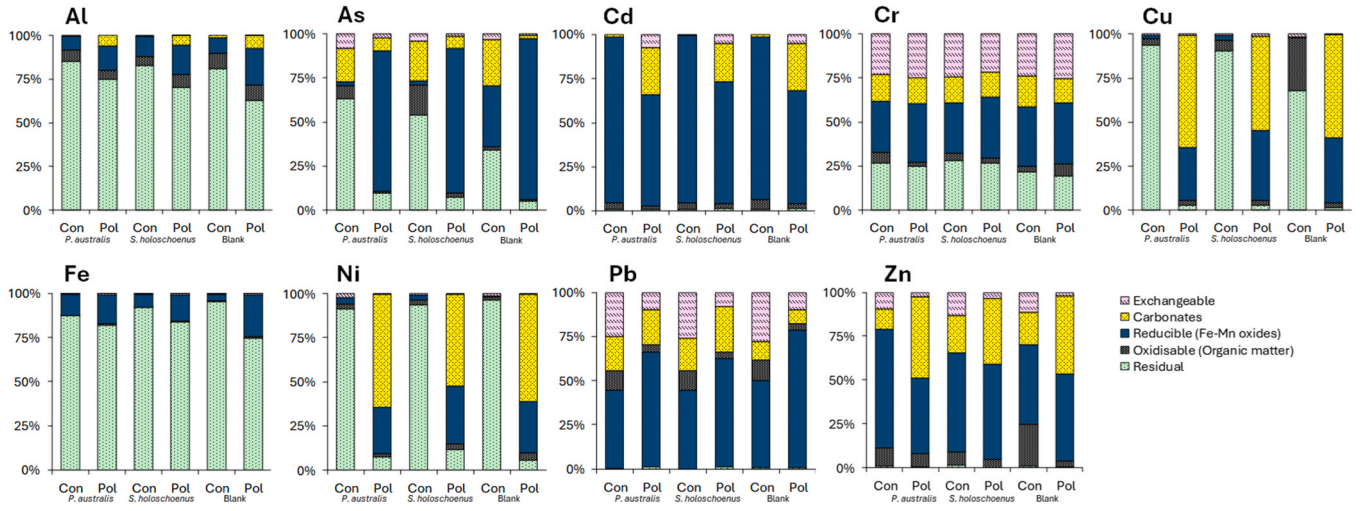

Fig. 1. Speciation of metals and metalloids in sediments (gravel) collected from the 4 L mesocosms of plants (*P. australis* and *S. holoschoenus*) and blanks (abiotic treatment without plants) at the end of the incubation period. "Con" and "Pol" at the x-axis represent the control (non-polluted water) and the polluted water treatments for incubations with plants (*P. australis* and *S. holoschoenus*) and without plants.

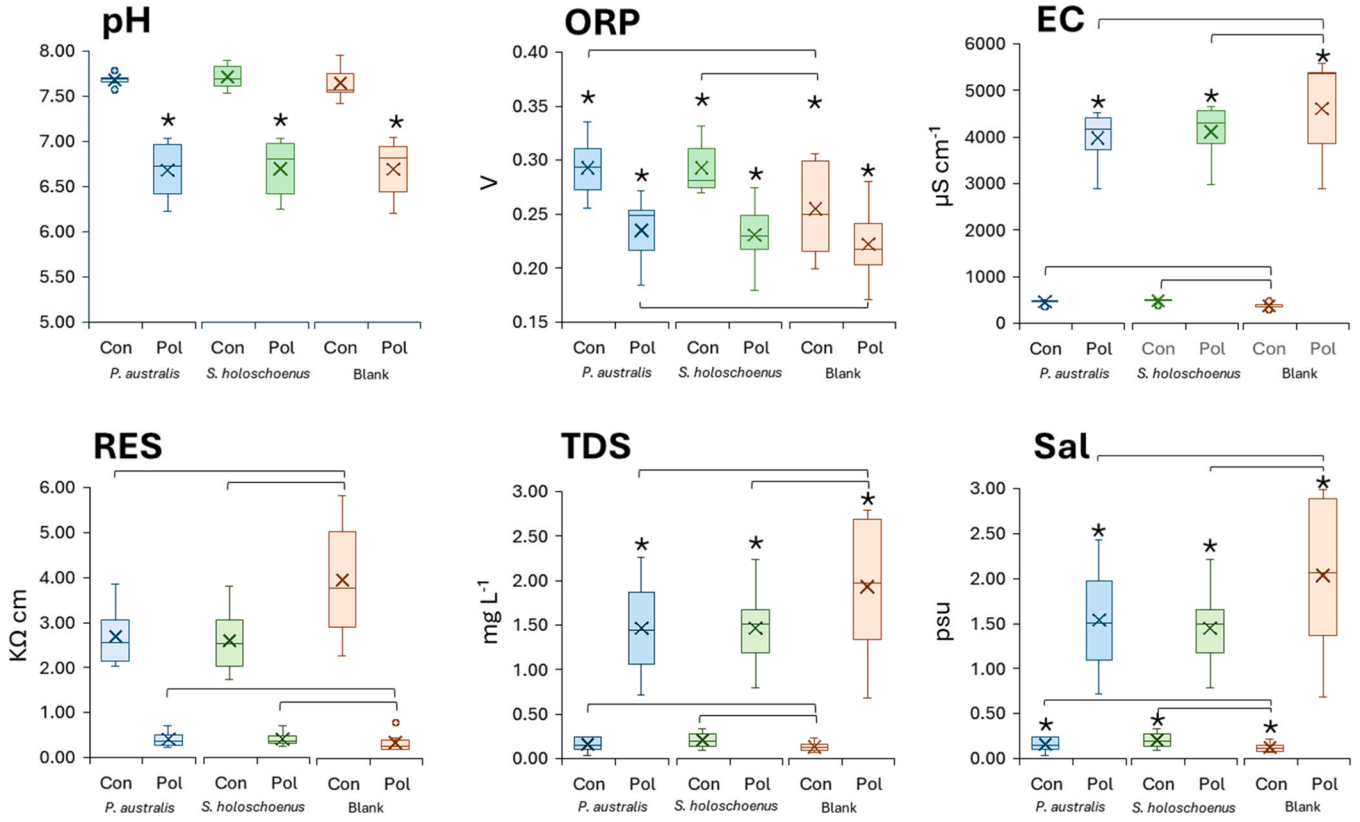

Fig. 2. Physical and chemical parameters of water analyzed and presented in box plots for the 4 L mesocosms of plants (*P. australis* and *S. holoschoenus*) and blanks (abiotic treatment without plants) during the incubation period (2 months). "Con" and "Pol" at the x-axis represent the control (non-polluted water) and polluted water treatments of *P. australis*, *S. holoschoenus*, and blanks (microsomes without plants). The bracket "⌐¬"on top of Cons' or Pols' bars indicates a significant difference ($p \leq 0.05$; repeated measures ANOVA) between plant and blank treatments, while the "*" indicates a significant difference ($p \leq 0.05$; repeated measures ANOVA) between the initial and the final time for the studied parameter.

water changed from initially 3.74 ± 0.09 to nearly 6 after addition to the 4-L mesocosm, to nearly 7.5–7.6 at the end of the experiment in both plant-based treatments (PBTs) and the control without plants (CWP). The ORP of the polluted water also changed from initially 0.28 ± 0.01 V, to ~0.17 V following addition to the 4-L mesocosms in both PBT and CWP and gradually increased to ~0.25 V for PBTs and ~0.28 V for CWP. For the EC, significant temporal variation was noted only in those treatments irrigated with polluted water; however, the variation was less marked in the PBT compared to the CWP mesocosms. In addition, significant differences were observed for EC, Res, TDS, and Sal between PBT and CWP, for both polluted and non-polluted water treatments. Values for EC, TDS, and Sal in water were significantly higher in polluted mesocosms for PBTs and CWP, while Res was significantly lower. In this manner, initial values were 2268.50 ± 68.59 μS cm^{-1} for EC, 0.44 ±0.01KΩ cm for Res, 1.13 ± 0.03 mg L^{-1} for TDS, and 1.17 ± 0.04 for Sal (Practical Salinity Use, PSU). By contrast, at the end of the exposure time the final values measured were for EC between 4199–4434 μS cm^{-1} for PBT and 3643 μS cm^{-1} for CWT, for Res between 0.69–0.71 KΩ cm for PBT and 0.77 KΩ cm for CWT, for TDS between 0.72–0.77 mg L^{-1} for PBT and 0.77 mg L^{-1} for CWT, and finally, for Sal (PSU) between 0.72–0.78 for PBT and 0.66 for CWT.

3.1.4. Metal and metalloid contents in plants

The metal and metalloid uptake profile of *P. australis* and *S. holoschoenus* is shown in Fig. 3. A clear trend to phytostabilization was observed when metals and metalloids were present, being more predominant in the case with metals having higher concentration in the polluted water. Generally, enhanced accumulation in the roots was observed for those metals with higher concentrations in the polluted water including Al, Cu, Fe, Ni, and Zn. In the case of As, Cd, Cr, significant concentrations were also reported for the aerial part, particularly for mesocosm exposed to the polluted water. For Pb there were no significant differences, neither between plants, nor between polluted treatments and non-polluted controls. Except for Cd (higher in shoots

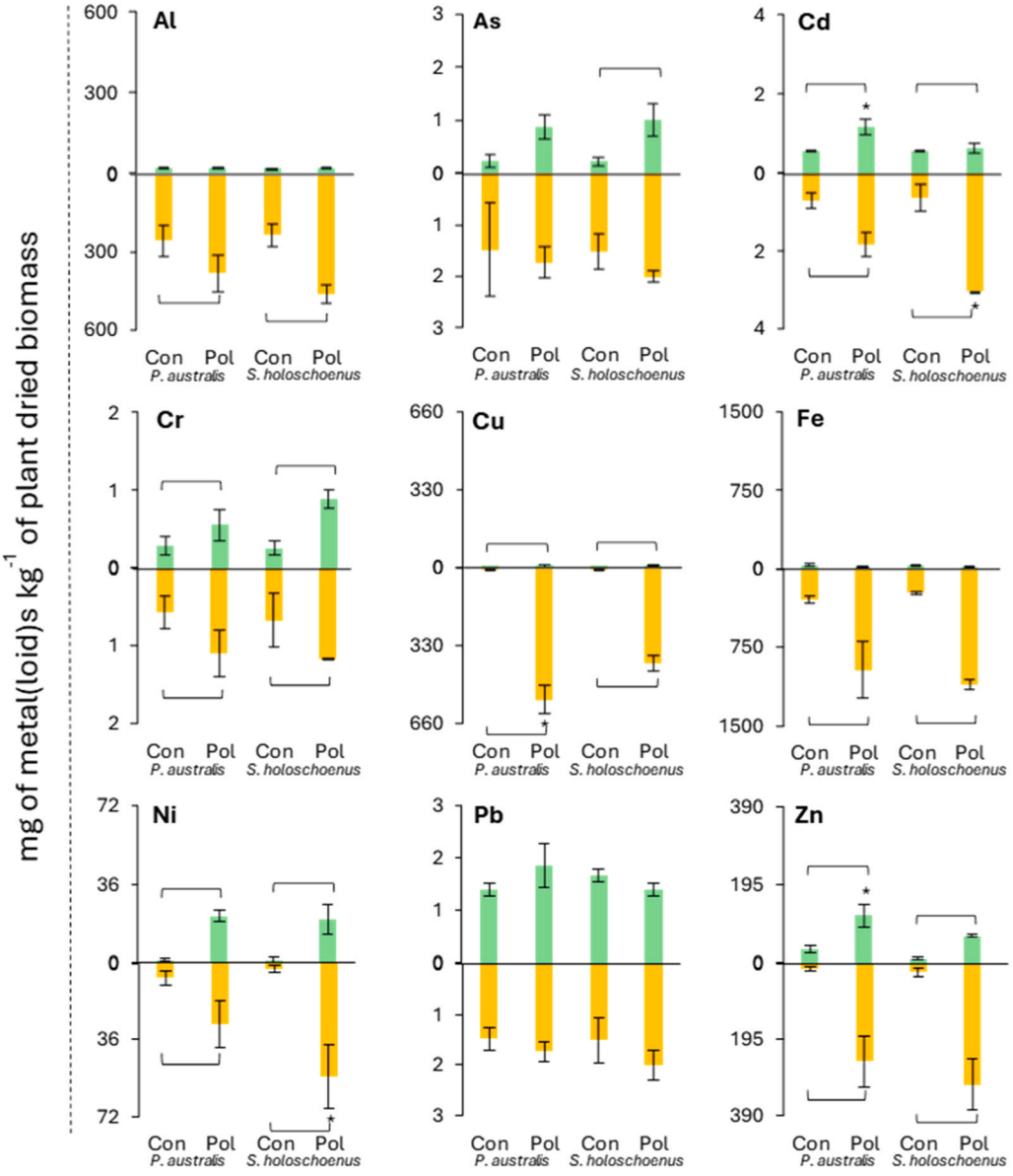

Fig. 3. Metal(loid)s compartmentalization in plants dried biomass in 4 L mesocosms. "Con" and "Pol" at x-axis represent the control (non-polluted water) and polluted water treatments for either *P. australis* or *S. holoschoenus*. The brackets "⌐¬"on top of Con and Pol bars indicate a significant difference ($p \leq 0.05$; one way ANOVA) between the exposure conditions within respective plants, while the "*" indicate the significant difference ($p \leq 0.05$) between the plants within the respective exposure condition.

Table 2
Plant and soil characteristics following harvest for the wetland mesocosm experiment.

Matrice and parameter*		*P. australis*			*S. holoschoenus*		
		Pro[1]	Acu[1]	Chr[1]	Pro[1]	Acu[1]	Chr[1]
Shoot (Stem + Leaves)	FW	20.75 ± 0.50 a	3.02 ± 0.54c	11.85 ± 1.58 b	24.79 ± 2.59 a*	13.33 ± 1.17 b*	19.18 ± 6.42 b*
	DW	5.55 ± 0.22 a	1.53 ± 0.19 b	5.16 ± 0.42 a	6.89 ± 1.03 ab*	5.11 ± 0.62 b*	8.46 ± 2.85 a*
	WC	15.20 ± 0.55 a	1.49 ± 0.43c	6.69 ± 1.77 b	17.90 ± 3.00 a	8.22 ± 1.07 b*	10.71 ± 3.59 b*
	IL	20.33 ± 5.22 a*	15.66 ± 4.25 b*	19.83 ± 4.52 a*	14.03 ± 2.29 a	12.90 ± 2.15 ab	12.17 ± 3.00 b
	FL	44.51 ± 8.39 b*	22.87 ± 6.17c*	51.58 ± 12.68 a*	21.20 ± 4.04 a	16.54 ± 2.88 b	22.60 ± 4.98 a
	CL	24.18 ± 7.44 b*	7.21 ± 4.68c*	31.74 ± 12.92 a*	7.16 ± 4.28 b	3.64 ± 3.27c	10.43 ± 4.93 a
Root	FW	33.13 ± 2.81 a*	9.87 ± 2.45c	29.81 ± 4.12 b	25.21 ± 2.24c	33.29 ± 14.83 b*	48.65 ± 20.44 a*
	DW	6.33 ± 0.74 a*	1.87 ± 0.38 b	8.08 ± 2.39 a	3.04 ± 0.32 b	4.50 ± 2.09 b*	6.72 ± 2.95 a
	WC	26.80 ± 2.56 a*	8.00 ± 2.51c	21.73 ± 1.90 b	22.16 ± 2.22 b	28.79 ± 13.41 b*	41.93 ± 18.29a*
	IL	16.36 ± 6.19 a	16.58 ± 5.18 a	16.28 ± 6.29 a	15.89 ± 4.40 a	18.83 ± 5.34 a	17.03 ± 4.54 a
	FL	30.71 ± 5.66 ab	27.65 ± 6.42 b	35.24 ± 13.41 a	28.49 ± 9.53 b	32.82 ± 13.97 b	60.34 ± 19.68 a*
	CL	14.35 ± 7.62 ab	11.07 ± 7.68 b	18.96 ± 13.66 a	12.60 ± 7.85 b	13.98 ± 13.73 b	43.32 ± 19.33 a*
Biomass (shoot)	C%	40.34 ± 0.48 a*	38.44 ± 1.17 b*	40.37 ± 0.58 a*	34.49 ± 2.58 a	33.31 ± 3.65 a	28.20 ± 5.61 a
	H%	6.19 ± 0.11 a*	6.00 ± 0.21 b*	6.17 ± 0.08 a*	5.59 ± 0.30 a	5.54 ± 0.38 a	5.05 ± 0.55 b
	N%	0.34 ± 0.08 b	0.74 ± 0.60 ab	1.12 ± 0.51 a	0.70 ± 0.56 a*	0.48 ± 0.26 a	0.82 ± 0.48 a
	O%	38.29 ± 0.99 a	35.78 ± 2.63 a	39.36 ± 3.89 a	43.13 ± 3.91 a*	40.80 ± 3.30 a*	37.89 ± 7.38 a
	HVV	17.15 ± 0.25 a*	16.57 ± 0.52 b*	17.07 ± 0.57 a*	13.88 ± 1.12 a	13.66 ± 1.95 a	11.64 ± 2.63 b
Growth substrate	Al	1095.05 ± 289.88 a	348.4 ± 99.27 b	543.37 ± 215.91 b	1159.38 ± 219.48 a	439.28 ± 51.57 b	461.59 ± 88.62 b
	As	2.08 ± 0.97 a	1.63 ± 0.75 ab	0.75 ± 0.26 b	2.25 ± 1.20 a	0.54 ± 0.21 b	0.33 ± 0.13 b
	Cd	22.65 ± 1.43 a	21.68 ± 1.23 a	8.03 ± 4.91 b	18.88 ± 6.17 a	2.62 ± 0.90 b	6.20 ± 5.46 b
	Cr	5.57 ± 2.04 a	3.76 ± 2.15 b	4.65 ± 2.39 ab	5.41 ± 1.79 a	3.32 ± 0.77 b	3.90 ± 1.60 b
	Cu	2006.72 ± 413.21 a	367.05 ± 73.31 b	637.73 ± 79.39 b	2074.55 ± 323.43 a	553.7 ± 101.07 b	503.23 ± 183.89 b
	Fe	2382.22 ± 508.55 a	1048.03 ± 413.32 b	1307.89 ± 314.66 b	2517.24 ± 511.94 a	1316.63 ± 469.86 b	1232.36 ± 418.74 b
	Ni	1688.62 ± 85.17 a	221.95 ± 22.69c	651.28 ± 160.95 b	1610.86 ± 127.86 a	297.26 ± 60.14c	890.26 ± 109.00 b
	Pb	3.37 ± 0.53 a	1.61 ± 1.19 b	2.31 ± 1.70 ab	4.42 ± 1.29 a	1.21 ± 0.80 b	2.45 ± 1.19 b
	Zn	772.9 ± 72.06 a	180.08 ± 40.16c	515.35 ± 89.59 b	687.69 ± 75.40 a	260.37 ± 40.88c	483.44 ± 55.56 b

* Parameters studied are abbreviated as FW = Fresh weight, DW = Dried weight, and WC = Water content in shoot, root, and soil (g), while IL = Initial length, FL= Final length, CL = Change in length noted for shoot and root (cm). For biomass the C% = Carbon%, H% = Hydrogen%, N = Nitrogen%, O = Oxygen%, and HHV = higher heating values (MJ of energy per kg^{-1} DW). Metal and metalloid contents in soil are presented in mg kg^{-1}. [1]Pro= Progressively-, Chr= Chronically-, and Acu= Acutely- exposed macrophyte populations irrigated with polluted water. Different letters between rows of the same species (a being significant higher followed by other alphabets), while * between same treatment displays significant statistical differences at $p < 0.05$.

than in roots for *P. australis*, and in roots than in shoots for *S. holoschoenus*) and Cu (higher in *P. australis* roots than in shoots), a similar metal(loid) uptake profile was observed for both plants. When irrigated with polluted water, the cumulative metal(loid) uptake was in decreasing order Fe > Cu > Al > Zn > Ni > Cd > Pb > As, and Cr.

3.2. Continuous exposure experiment in wetland mesocosms

3.2.1. Plant physiology

The data for plant biomass production is shown in Table 2. In general, plants cultivated under Pro and Chr exposure exhibited greater tolerance to pollutants than those under Acu exposure. This was particularly evident in terms of shoot and root characteristics, as assessed by means of fresh and dry weight, water content, initial and final length as well as change in length, particularly for *P. australis*. For *S. holoschoenus*, however, the greatest root development occurred under the Chr regime, followed by the Acu and Pro regimes.

Shoot fresh weight, water content, final length, and changes in length were significantly higher for both plants in Pro exposure, in comparison to Acu and Chr exposure. The shoot dried weight (SDW) for *S. holoschoenus* was significantly higher in Chr (8.46 ± 2.85 g), followed by Pro and Acu, while with *P. australis* the SDW was higher in Pro (5.55 ± 0.22 g) and Chr (5.16 ± 0.42 g) compared to Acu (1.53 ± 0.19 g). The root fresh weight (RFW; 33.13 ± 2.81 g), dried weights (RDW; 6.33 ± 0.74 g), and the water content (RWC; 26.80 ± 2.56 g) for *P. australis* were significantly higher under Pro exposure, followed by Chr and Acu. By contrast, higher RFW, RDW, and RWC were measured in Chr for *S. holoschoenus,* 48.65 ± 20.44, 6.72 ± 2.95, and 41.93 ± 18.29, respectively. The root FL and CL for both plants were noted significantly higher in Chr, with *S. holoschoenus* showing higher root lengths (FL = 60.34 ± 19.68 and Cl = 43.32 ± 19.33), compared to *P. australis* (35.24 ± 13.41 and 18.96 ± 13.66, root FL and CL, respectively).

The elemental composition (C, H, N and O) and higher heating values (HHV) of the plants are presented in Table 2. For *P. australis*, the HHV was highest under the Pro and Chr exposure regimes compared to the Acu regime, whereas for *S. holoschoenus* the HHV was highest under the Chr exposure regime, followed by the Acu and Pro regimes. Concomitantly, plants with higher HHV showed a greater relative abundance of C, H and O, but not necessarily N. *P. australis* showed a greater HHV than *S. holoschoenus* under all exposure regimes. The higher C%, H%, and HHV were noted in *P. australis*, in comparison to *S. holoschoenus,* within all exposure regimes. With reference to C%, the higher contents were noted in Pro (40.34 ± 0.48) and Chr (40.37 ± 0.58), compared to Acu (38.44 ± 1.17) in *P. australis*, while with the *S. holoschoenus* the C% of Pro (34.49 ± 2.58) and Acu (33.31 ± 3.65) were significantly higher than Chr (28.20 ± 5.61). Similarly, the H% were higher in Pro and Chr, than Acu for *P. australis,* while for *S. holoschoenus* the H% contents were higher in Pro and Acu, compared to Chr. The N% of *S. holoschoenus* (0.70 ± 0.56) in Pro was significantly higher than that of *P. australis* in the same exposure regime, while no significant differences were noted between plants exposed with Acu or Chr. There was no significant difference in the O% for both plants with reference to difference exposure types. The HHV was found highest for *P. australis* biomass, in all the exposure regimes (MJ of energy kg^{-1}) compared to the *S. holoschoenus* biomass, with significantly higher HHV in Pro and Chr (17.15 ± 0.25 and 17.07 ± 0.57), followed by Acu (16.57 ± 0.52). While, for *S. holoschoenus* biomass, the higher HHVs were noted in Pro and Acu (13.88 ± 1.12 and 13.66 ± 1.95, respectively) compared to Chr (11.64 ± 2.63).

3.2.2. Water physico-chemical parameters

The physico-chemical parameters of polluted water for the wetland mesocosm experiment are presented in supplementary figure 3. In general, the quality of the polluted water as assessed by pH, ORP, EC, RES, TDS, and Sal were similar in the plant mesocosms. Only the pH of the water in *S. holoschoenus* mesocosms (6.1 – 7.1 units) was slightly more acidic than in *P. australis* mesocosms (6.8 – 7.2 units). The ORP range was higher under Pro and Chr exposure regimes compared to the Acu, whereas the opposite trend was observed for EC. The pH range under Acu exposure was slightly higher (more basic) for *P. australis* mesocosms than under the Pro and Chr exposure regimes. The differences show some trends, but they were not statistically assessed. No evident effects due to the exposure regime were observed for the parameters RES, TDS and Sal. Among the parameters studied, changes were observed with reference to the exposure regime and plant type.

The PCA of the parameters with reference to different exposure regimes resulted in extraction of 2 principal components (PCs) with eigenvalues > 1 for Pro, 3 PCs for Acu, and 3 PCs with Chr (Supplementary Table 1S). Besides, the chosen PCs have eigenvalue higher than 1, the scattering plots were constructed only with the initial 2 PCs, accounting more than 70% of variance, and are presented in Fig. 4. The cumulative percentage variance of the first 2 PCs for Pro, Acu, and Chr was 72.28, 80.94, and 72.41, respectively. With reference to different exposure regimes, it was identified that for progressive exposure (Pro) the pH, EC, TDS, and Sal were in PC1, with eigenvalue of 3.884, contributing higher to the data variability (55.49%), while the influence of plant type, ORP, and RES were in PC2 (eigenvalue 1.176) with contribution to data variance of 16.79%. In the acute exposure regime, the EC, ORP, TDS, and Sal were in PC1 (eigenvalue 4.099) with a contribution to data variability of 58.55%, while pH, RES, and plant type were in PC2 (eigenvalue 1.568) with a data variability contribution of 22.38%. However, in chronic exposure regime (Chr) the role of plant type was in PC1 (eigenvalue 3.938), along with EC, ORP, TDS, and SAL, contribution 56.25% in data variability, while pH and Res were in PC2 (eigenvalue 1.131) with a contribution to data variability of 16.15%.

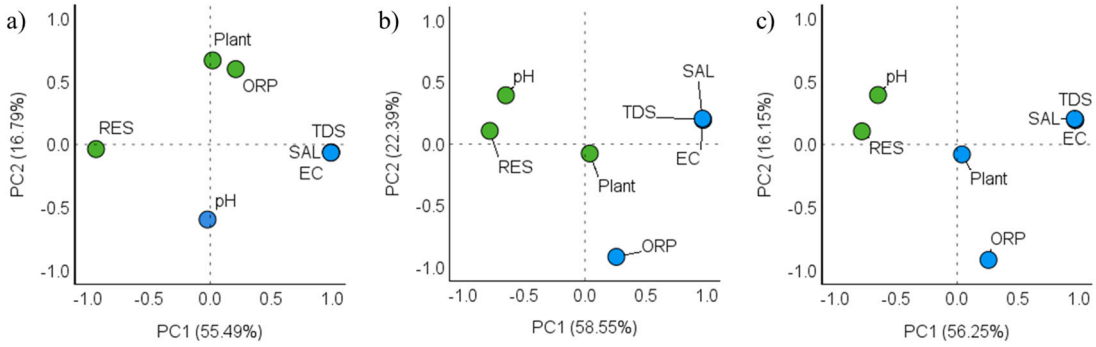

Fig. 4. Principal component analysis on the data for water parameters and plants. a) progressively exposed population (Pro), b) acutely exposed population (Acu), and c) chronically exposed population (Chr). The blue parameters have significantly higher loading values in principal component 1, while the green parameters have significantly higher loading values in principal component 2.

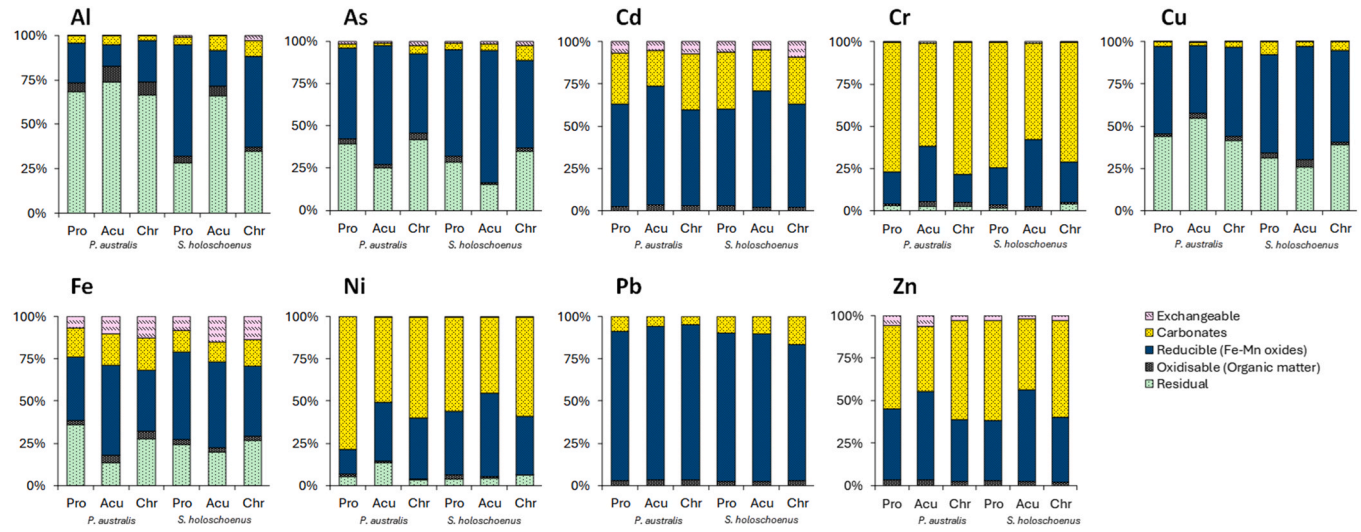

Fig. 5. Speciation of metals and metalloids in sediments (gravel) collected from the wetland mesocosm plants (*P. australis* and *S. holoschoenus*) under different exposure regimes at the end of the incubation period. "Pro", "Acu", and "Chr" at x-axis represent the progressive, acutely, and chronically exposed population of *P. australis* and *S. holoschoenus*.

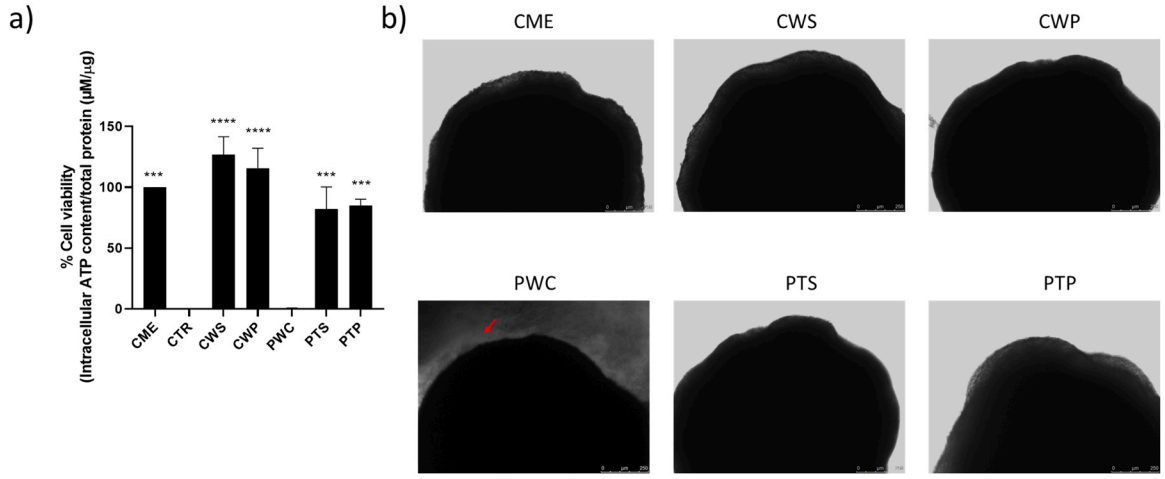

Fig. 6. HepG2 spheroid viability. a) The graph represents the relative intracellular ATP content in liver spheroids after a 24-hour treatment with water samples, determined using the ATP assay and normalized to total protein content. Three independent experiments were performed, and at least four spheroids from each bioreactor were collected. Results are presented as the mean ± SEM of relative μM ATP/μg protein, normalized to the technical control (CME). b) Morphological boundaries of spheroids under each condition. The red arrow indicates disaggregation of cells exposed to polluted water. CME: control cell media; CTR: death control (10% Triton X-100); CWS: control water *Scirpus holoschoenus*; PWC: control water polluted without treatment; PTS: polluted treated water *Scirpus holoschoenus*; PTP: polluted treated water *Phragmites australis*. Scale bar: 250 μm. Differences were analyzed using one-way ANOVA followed by a Dunnet multiple comparisons test, with significance set at $p \leq 0.05$.

3.2.3. *Metal and metalloid contents in growth substrate and plants*

The total GS metal(loid) content about the exposure regime is presented in Table 2. Significantly higher concentrations of all metal(loid)s (mg kg^{-1}) in GS were observed for both plant treatments under Pro exposure compared to Acu and Chr. For *P. australis* and *S. holoschoenus* cultivated in Pro regime the metal(loid)s content (mg kg^{-1}), which were very high, are as follows (alphabetically) Al (1095.05 ± 289.88 and 1159.38 ± 219.48), Cu (2006.72 ± 413.21 and 2074.55 ± 323.43), Fe (2382.22 ± 508.55 and 2517.24 ± 511.94), Ni (1688.62 ± 85.17 and 1610.86 ± 127.86), and Zn (772.9 ± 72.06 and 687.69 ± 75.40). Concentrations in the GS were approximately in the range 300 – 2000 mg/kg for Fe, Cu, Ni, Al and Zn, 2.6 – 23 mg/kg for Cd and 0.5 – 5.4 for Pb, Cr and As for both plant treatments. The extent of the metal(loid) adsorption in GS was similar for both plants, but slightly different between exposure regimes. In this manner, metal(loid) concentrations in GS followed the order Fe > Cu > Ni > Al > Zn > Cd > Pb > Cr > As - under Pro exposure, Fe > Cu > Al > Ni > Zn > Cd > Cr > Pb, and As - under Acu exposure, and Fe > Ni > Cu >Al > Zn > Cd > Cr > As, and Pb - under Chr exposure.

The compartmentalization of metals and metalloids in the roots and shoots of *P. australis* and *S. holoschoenus* in the wetland mesocosms was very similar to that observed in the 4 L mesocosms (supplementary figure 4). Generally, the concentrations of metals and metalloids in the roots of both plants were significantly higher than in the shoots, except for As, and to a lesser extent, Cr and Pb, where the concentrations were comparable. The concentration of metals and metalloids in the roots of both plants correlated with the respective concentrations initially present in the polluted water. Consequently, the highest concentrations in the roots were recorded for the elements with the highest concentrations in the polluted water: Al, Cu, Fe, Ni, and Zn. The concentrations of elements in the shoots were comparatively negligible.

In general, metal(loid) speciation in GS was element-dependent,

meaning that distinctive speciation patterns were observed depending on the element. These patterns were generally more evident than the effects of potential speciation due to plant or exposure treatment (Fig. 5). In this manner, Cd and Pb were primarily associated with Fe- and Mn-oxides, and to a lesser extent with carbonates. In contrast, Cr, Ni, and Zn were primarily associated with the carbonate fraction, followed by the Fe- and Mn-oxide fraction. Al, As, and Cu speciation mainly occurred within the Fe- and Mn-oxide and the residual fractions, whereas Fe exhibited the most varied speciation of all the elements. Iron was present in all fractions, with the lowest association with the organic fraction. In terms of exposure regime, the speciation of the elements Cd, Cr and Zn within the Fe- and Mn-oxide fraction was over 10% higher under Acu exposure than under Pro and Chr exposure. The most relevant difference for the plants was observed for Al, which was found to be significantly more highly associated with the Fe- and Mn-oxide fraction relative to the residual fraction in *S. holoschoenus* mesocosms than in *P. australis* mesocosms under Pro and Chr exposure.

3.3. Effect of Groundwater Phytoremediation on the Viability of Mature HepG2 Spheroids

The viability of the HepG2 hepatocellular carcinoma cell line was assessed to determine the maximum suitable water dosage for evaluating potential oral human health effects, as well as to compare toxicity levels before and after phytoremediation (Fig. 6a). After 24 h of exposure, the polluted water control (PWC) resulted in almost total loss of cell viability, which was similar to the death control (CTR), which contained 10% Triton X-100. In contrast, the non-polluted control without plants (CME) (representing 100% cell viability) and the non-polluted water control treatments with plants (CWS for *S. holoschoenus* and CWP for *P. australis*), showed no reduction in cell viability. The treatment of the polluted groundwater using *Phragmites australis* and *Scirpus holoschoenus* (designated as PTP and PTS, respectively) significantly improved cell viability compared with PWC, reaching values over 75% cell viability, which is considered non-toxic. There were no significant differences in performance between the two plant treatments, neither for the controls without polluted water (CWS and CWP) nor for the ones with polluted water (PTS and PTP) with and without polluted water.

Regarding the liver spheroid morphology depicted in Fig. 6b, the constructs exhibited a well-defined boundary in all treatments, except for PWC where the cells appeared detached from the spheroid core and dead, as shown in Fig. 6a, likely due to exposure to the polluted water. The results indicate that mesocosms planted with *P. australis* and *S. holoschoenus* effectively removed metals and metalloids from contaminated groundwater, thereby enhancing water quality and rendering the treated water compatible with cell survival. The comparable efficacy observed between the two species suggests that both are viable options for phytoremediation in similar contexts. Overall, these findings reinforce the potential of phytoremediation as a sustainable and effective strategy for groundwater decontamination with positive implications for human health, addressing an important environmental and public health challenge.

4. Discussion

Polluted groundwater poses a significant risk to both drinking water resources and hydraulically connected surface water bodies [13]. Macrophyte-based phytoremediation can provide a nature-based solution for treating contaminated groundwater either in constructed wetland systems or in situ in areas where vegetation grows along the affected surface water bodies [37,38]. However, the potential of macrophytes for phyto-treatment depends on the type of plant, contaminant type and concentration, and the exposure regime (acute, progressive, or chronic). The physiological response of plants (*Phragmites australis* and *Scirpus holoschoenus*) exposed to metal(loid)s containing groundwater in the acute experiment (4 L batch mesocosms) demonstrated strong tolerance. Both plants managed to maintain biomass and photosynthetic pigments that are comparable to control plants. This indicates the tolerance of both species to the multi-metal(loid) contamination. These findings are consistent with previous studies highlighting the tolerance of *P. australis* to various heavy metals through mechanisms such as pollutant exclusion, phytostabilization, and increased root growth, which enhances the surface area of contact with the contaminated substrate [21]. Previous work has also shown that *S. holoschoenus* exposed to polluted water can exhibit increased shoot biomass and tissue water content, suggesting mechanisms that enhance water uptake and biomass production, enabling dilution of pollutants within plant tissues [11]. However, prolonged exposure to polluted groundwater could lead to phytotoxic effect.

Metal(loid)s contamination soil, sediment, or growth substrate can influence soil health by affecting microbial processes and rhizospheric enzymatic activities [37,39]. In the present study, several enzymatic activities increased in the acute exposure experiment, such as AcPA and bNAG in the *P. australis* treatment, indicating possible microbial adaption or changes in nutrient cycling in response to pollutants. In contrast, significantly lower enzyme activities in the *S. holoschoenus* treatment suggest an induced inhibitory effect on the rhizospheric microbial community. The presence of metal(loid)s is known to alter the rhizospheric enzyme activities by inhibiting the microbial population and reducing root exudation and growth [40]. These responses may also be influenced by changes in the environmental conditions, such as physico-chemical parameters pH, electrical conductivity, soil composition, and organic matter [12,41,42].

A significant accumulation of metals in growth substrate was observed in all 4 L mesocosms exposed to the polluted water with high metal load, particularly for Cu, Fe, Ni, and Zn. Consequently, significant uptake and accumulation occurred in the roots of both plants, indicating a phytostabilization rather than a phytoextraction mechanism. Root accumulation driven by increasing metal(loid)s levels in water and soil/substrate is desirable for phyto-attenuation/-stabilization as it minimizes transfer of contaminants to aerial plant tissues [43,44]. A significant increase in the pH of the water (from acidic to near neutral) was observed across all mesocosms by the end of the two-month experiment. This pH shift occurred in both planted and unplanted systems, indicating an abiotic baseline contribution to the metal(loid) attenuation through chemical precipitation. However, the planted mesocosms exhibited significantly lower EC, TDS, and Sal compared to the unplanted mesocosms, suggesting an additional vegetation-mediated removed the residual dissolved solid. Changes in metal(loid) fractionation in GS were observed in the planted mesocosms, particularly for Al, As, Fe, Pb, and Zn, indicating the influence of rhizospheric process such as root exudation, organic matter incorporation, and rhizospheric microbiome changes [11,15,32]. Therefore, it indicates that the abiotic pH shifts can initiate the remediation process, however plants play a pivotal role in enhancing and sustaining the metal and metalloid removal which ensures the long-term stabilization of sequestered elements. Wetland systems involve complex interactions between biotic and abiotic geochemical processes that affect pH and the solubility of elements such as Al and Fe [40,45]. The higher Fe concentration in the tested polluted water likely contributed to the fractionation of various elements, including As, Cd, Cr, Cu, Ni, Pb, and Zn, within the Fe- and Mn-oxides fraction.

Using appropriate macrophytes is critical for large-scale phytoremediation applications [10]. Short-term treatability tests allow rapid screening of suitable plants before longer-term testing under larger treatment volumes [11,12]. However, aquatic plants in natural systems are more often exposed gradually and continuously to contaminates through non-point pollution sources and flowing water [6,14]. Therefore, it is crucial to determine the effects of different exposure regimes to evaluate the potential of phytoremediation approaches using macrophytes. In the study, plants exposed to progressive and chronic regimes

generally showed greater tolerance than those exposed to acute conditions, particularly in terms of plant growth. Previous studies have shown that gradual exposure to acidic and metal(loid) contaminated water can lead to the development of tolerance, whereas acute exposure may induce plant stress even when metal(loid) mobilization or uptake remains limited [11,41,45]. Therefore, Pro and Chr exposure allows plants to acclimatize to polluted environments and maintain biomass production [38,46].

The metal(loid) uptake profile in the continued exposure wetland experiment, was similar as of the acute experiment, showed preferential accumulation of metal(loid)s in roots except for As, and to a lesser extent Cr and Pb. These elements together with Cd, were at lower concentration in the polluted water and GS, which may explain the smaller difference between roots and shoots concentrations. For elements at high concentrations, the metal(loid) accumulation occurred more mainly in the roots than in aerial tissues. Hamidian et al. [20] also reported that *P. australis* growing on Shoor River, Iran, accumulated higher metal (loid)s in root compared to aerial parts, when the concentration of metal (loid)s in sediments was found in following order Al > Fe > Mn > Zn > Mg > Ni > Cr > Pb > Cu > As > V. Similarly, significant phytoattenuation and metal(loid) accumulation was observed in roots for *S. holoschoenus* growing on highly acidic water (pH 2–3) and sediments of Água Forte and the Roxo streams, Portugal [22]. Apart from the evident preferential metal(loid) accumulation in the roots, no consistent pattern was observed regarding the influence of the exposure regime or the plant species on metal(loid) distribution within plant tissues. This suggests that continued exposure may stabilize metal(loid) uptake patterns over time, as previously reported in studies with different incubation periods. Khan et al. [47] reported that *S. holoschoenus*, when irrigated with polluted groundwater at different hydraulic retention times (15 and 30 days) showed fluctuations in the metal(loid)s uptake and compartmentalization.

Analysis of total metal(loid)s in GS under continuous exposure showed the highest accumulation in the Pro exposure treatment. This was attributed to the gradual increase in pollutant concentration from the continued addition of contaminated groundwater, which promoted stabilization of trace elements onto the growth substrate and rhizosphere [45]. Overall, the exposure regime and the plant species had a limited effect on metal(loid) speciation compared with the nature and concentration of the element after continued exposure. These results highlight the dynamic interplay between plant activity, exposure duration, organic matter, redox fluctuation, anoxic/oxic conditions, and metal speciation [48,49]. The polluted groundwater phytoremediation for long term continuous exposure by *P. australis* and *S. holoschoenus*, not only helps in the pollutants' remediation, but also improves water quality, as reflected by a significant enhancement of the viability of mature HepG2 spheroids. The recovery in cell viability after phytoremediation provides convincing evidence for the potential of these plants to mitigate the harmful effects of the polluted water on human health. The finding links the ecological benefits of phytoremediation to tangible improvements in water quality, as indicated by the reduction in the treated-water cytotoxicity to HepG2 cells.

In phytoremediation systems, harvested biomass containing metal (loid)s may require management after treatment. Biomass valorization via incineration is among the commonly adopted practices to manage plant residues [50,51]. The assessment of the biomass for bioenergy potential showed higher carbon content (%) and HHV in *P. australis* compared with *S. holoschoenus*. A feedstock with a calorific value of 15–17 MJ kg^{-1} is considered marginally good for biomass energy production or fuel generation. Such calorific values are comparable with feedstock such as rice straw (~15.8 MJ kg^{-1}) and low-grade coal (~17–23.2 MJ kg^{-1}) [26,52]. In this study, the HHV of *P. australis* reached 17.15 ± 0.25 MJ kg^{-1} under progressive exposure, indicating the potential of energy recovery after phytoremediation. However, variations in these parameters across the exposure regimes indicate that pollutant exposure can influence the biochemical composition and calorific values of the plant biomass.

This work presents a concrete foundation to use the potential aquatic plants *P. australis* and *S. holoschoenus* for an extended and sustainable remediation option for metal(loid)-polluted water bodies. However, more detailed investigations are needed to quantify the role of such parameters and complexity of natural wetland environment, as these aspects can impact on the NBS-based remediation and metal(loid)s long-term fate and bioavailability [14,39,49]. The proceeding studies to this work should focus on the scaling up the mesocosm studies to pilot-scale constructed wetlands by evaluating the performance of plant species under more realistic field conditions, considering factors like seasonal variations, hydraulic loading rates, long-term accumulation of pollutants, and global changes. Evaluating the environmental footprint, life cycle analysis, costing and impacts, including energy consumption, greenhouse gas emissions, and waste generation, to ensure its true sustainability compared to conventional remediation methods.

5. Conclusion

To mitigate the risks posed by complex multi-metal(loid) contamination in groundwater, nature-based solutions using aquatic plants represent a sustainable, dual-purpose strategy for detoxification and simultaneous environmental restoration. This research establishes a unique framework for evaluating the resilience of phytoremediation systems by shifting focus from static assessments to dynamic regimes (acute, progressive, and chronic). This study demonstrates that exposure dynamics are a critical determinant of macrophyte performance. Based on the evidence of superior biomass production and pollutant removal observed under progressive and chronic exposure, the study suggests that the gradual acclimatization of macrophytes (biological priming) is pivotal for the long-term sequestration capacity of large-scale constructed wetlands. Furthermore, the successful recovery of HepG2 cell viability due to removal of metal(loid)s and stabilization of water physical parameters (notably pH), affirms the efficacy of macrophyte-based remediation in effectively removing the pollutant and mitigating the human health risk. It highlights the necessity of integrated testing, monitoring both pollutant removal and ecotoxicity reduction, to ensure robust nature-based remediation outcomes and prevent cascading failures. Finally, this study confirms the potential of post-phytoremediation biomass valorization, supporting bioresource recovery. These findings provide a sound scientific foundation for deployment of macrophyte assisted phytoremediation to tackle the global challenge of groundwater restoration.

Environmental Implications

Groundwater polluted with metal(loid)s and hydraulically connected to surface watercourses may pose a significant environmental and economic threat to freshwater ecosystems and catchment areas, depending on seasonal hydrological fluctuations. Using macrophyte plants for phytoremediation/attenuation offers an attractive, nature-based approach to mitigating the effects of pollutants entering freshwater systems from groundwater. To validate their phytoremediation potential, *P. australis* and *S. holoschoenus* were subjected to variable exposure regimes involving polluted groundwater. Our study shows that both plant species can be successfully incorporated into phytoremediation strategies for water contaminated by multiple metals and metalloids under changing conditions, as represented by different exposure regimes.

CRediT authorship contribution statement

Laura Gómez-Cuadrado: Methodology, Formal analysis. **Dalia de la Fuente-Vivas:** Methodology, Formal analysis. **Herwig De Wilde:** Resources, Formal analysis. **Gonzalo Salazar-Mardones:** Validation, Resources. **Rocío Barros:** Writing – review & editing, Visualization,

Project administration, Methodology, Funding acquisition, Conceptualization. **Alfredo Pérez-de-Mora:** Resources, Project administration, Formal analysis. **Aqib Hassan Ali Khan:** Writing – review & editing, Writing – original draft, Visualization, Validation, Supervision, Software, Investigation, Formal analysis, Data curation, Conceptualization. **Carlos Rad:** Writing – review & editing, Writing – original draft, Validation, Methodology, Formal analysis. **Alberto Soto-Cañas:** Writing – original draft, Validation, Software, Methodology, Investigation, Formal analysis. **Blanca Velasco-Arroyo:** Resources, Project administration, Methodology, Funding acquisition. **Andrea Martin-Pablo:** Methodology, Investigation, Formal analysis.

Declaration of Generative AI and AI-assisted technologies in the writing process

During the preparation of this work the authors used Gemini by Google to improve readability and language used in some parts of the review. After using this tool, the authors reviewed and edited the content as needed and authors take full responsibility for the content of the publication.

Declaration of Competing Interest

The authors declare the following financial interests/personal relationships which may be considered as potential competing interests. Rocio Barros reports financial support was provided by European Union. Alberto Soto-Cana reports financial support was provided by Junta de Castilla y León. If there are other authors, they declare that they have no known competing financial interests or personal relationships that could have appeared to influence the work reported in this paper

Acknowledgments

Open access funding provided by UNIVERSIDAD DE BURGOS. Authors also acknowledge BIOSYSMO funding received to carry out this research work. BIOSYSMO project is funded by the European Union under Grant Agreement No. 101060211. AS and A M-P has a predoctoral grant of Junta de Castilla y León (ORDEN EDU/842/2022, de 6 de julio).

Appendix A. Supporting information

Supplementary data associated with this article can be found in the online version at doi:10.1016/j.jhazmat.2026.142030.

Data availability

Data will be made available on request.

References

[1] Väänänen, K., Leppänen, M.T., Chen, X.P., Akkanen, J., 2018. Metal bioavailability in ecological risk assessment of freshwater ecosystems: From science to environmental management. Ecotoxicol Environ Saf 147, 430–446. https://doi.org/10.1016/J.ECOENV.2017.08.064.

[2] Magesh, N.S., Tiwari, A., Botsa, S.M., da Lima Leitao, T., 2021. Hazardous heavy metals in the pristine lacustrine systems of Antarctica: Insights from PMF model and ERA techniques. J Hazard Mater 412, 125263. https://doi.org/10.1016/J.JHAZMAT.2021.125263.

[3] Wu, J., Jiang, J., Xu, C., Cai, Y., Li, M., Yang, Y., Zhang, S., 2024. A comprehensive assessment of heavy metals, VOCs and petroleum hydrocarbon in different soil layers and groundwater at an abandoned Al/Cu industrial site. Ecotoxicol Environ Saf 284, 116927.

[4] Khalijian, A., Lorestani, B., Sobhanardakani, S., Cheraghi, M., Tayebi, L., 2022. Ecotoxicological assessment of potentially toxic elements (as, cd, Ni and V) contamination in the sediments of southern part of Caspian Sea, the case of Khazar Abad, Mazandaran Province, Iran. Bull Environ Contam Toxicol 109, 1142–1149.

[5] Wang, X., Shen, T., Yang, W., Kang, L., Li, B., Tian, Y., Li, J., Zhang, L., 2024. A critical review on the application of pyrite in constructed wetlands: Contaminants removal and mechanism. J Water Process Eng 63, 105353. https://doi.org/10.1016/J.JWPE.2024.105353.

[6] Zhou, L., Zhao, X., Teng, M., Wu, F., Meng, Y., Wu, Y., Byrne, P., Abbaspour, K.C., 2023. Model-based evaluation of reduction strategies for point and nonpoint source Cd pollution in a large river system. J Hydrol 622, 129701. https://doi.org/10.1016/J.JHYDROL.2023.129701.

[7] Alghanem, S.M.S., Alsudays, I.M., Farid, M., Sarfraz, W., Ishaq, H.K., Farid, S., Zubair, M., Khalid, N., Aslam, M.A., Abbas, M., Abeed, A.H.A., 2024. Evaluation of heavy metal accumulation and tolerance in oxalic acid-treated *Phragmites australis* wetlands for textile effluent remediation. Int J Phytoremediat 26, 2048–2063. https://doi.org/10.1080/15226514.2024.2372849.

[8] Talpur, H.A., Talpur, S.A., Mahar, A., Rosatelli, G., Baloch, M.Y.J., Ahmed, A., Khan, A.H.A., 2024. Investigating drinking water quality, microbial pollution, and potential health risks in selected schools of Badin city, Pakistan. HydroResearch 7, 248–256. https://doi.org/10.1016/j.hydres.2024.04.004.

[9] Selahvarzi, S., Sobhan Ardakani, S., 2022. Analysis and health risk assessment of toxic (Cd and Pb) and essential (Cu and Zn) elements through consumption of potato (*Solanum tuberosum*) cultivated in Iran. Int J Environ Anal Chem 102 (18), 6310–6320. https://doi.org/10.1080/03067319.2020.1807974.

[10] Rai, P.K., 2019. Heavy metals/metalloids remediation from wastewater using free floating macrophytes of a natural wetland. Environ Technol Innov 15, 100393. https://doi.org/10.1016/J.ETI.2019.100393.

[11] Velasco-Arroyo, B., Curiel-Alegre, S., Khan, A.H.A., Rumbo, C., Pérez-Alonso, D., Rad, C., De Wilde, H., Pérez-de-Mora, A., Barros, R., 2024. Phytostabilization of metal(loid)s by ten emergent macrophytes following a 90-day exposure to industrially contaminated groundwater. N Biotechnol 79, 50–59. https://doi.org/10.1016/J.NBT.2023.12.003.

[12] Khan, A.H.A., Velasco-Arroyo, B., Rad, C., Curiel-Alegre, S., Rumbo, C., de Wilde, H., Pérez-de-Mora, A., Martel-Martín, S., Barros, R., 2024. Metal(loid) tolerance, accumulation, and phytoremediation potential of wetland macrophytes for multi-metal(loid)s polluted water. Environ Sci Pollut Res 31, 65724–65740. https://doi.org/10.1007/S11356-024-35519-5.

[13] Xiang, S., He, X., Yang, Q., Wang, Y., 2024. Migration and natural attenuation of leachate pollutants in bedrock fissure aquifer at a valley landfill site. Environ Poll 362, 124963. https://doi.org/10.1016/J.ENVPOL.2024.124963.

[14] Hussain, H., Mahmood, S., Khalid, A., Shahzad, K., Anjum, M.Z., 2023. Seasonal variation in non-point source heavy metal pollution in Satpara Lake and its toxicity in trout fish. Environ Monit Assess 195, 901. https://doi.org/10.1007/s10661-023-11498-x.

[15] Khan, A.H.A., Budzyńska, S., Zine, H., Vázquez-Núñez, E., Talpur, S.A., Hassan, M., Barros, R., 2025. Dendroremediation: A sustainable nature-based solution for management of abandoned mining sites and brownfields. J Clean Prod 501, 145342. https://doi.org/10.1016/J.JCLEPRO.2025.145342.

[16] Fan, M., Xia, P., Chen, W., Wang, T., Du, X., Lin, T., 2021. Metal(loid) accumulation levels in submerged macrophytes and epiphytic biofilms and correlations with metal(loid) levels in the surrounding water and sediments. Sci Total Environ 758, 143878. https://doi.org/10.1016/J.SCITOTENV.2020.143878.

[17] Li, C., Wang, H., Liao, X., Xiao, R., Liu, K., Bai, J., Li, B., He, Q., 2022. Heavy metal pollution in coastal wetlands: A systematic review of studies globally over the past three decades. J Hazard Mater 424, 127312. https://doi.org/10.1016/J.JHAZMAT.2021.127312.

[18] Polechońska, L., Klink, A., 2023. Macrophytes as passive bioindicators of trace element pollution in the aquatic environment. Wiley Interdiscip Rev Water 10, e1630. https://doi.org/10.1186/S13765-020-0493-6.

[19] Serafini, R.J.M., Arreghini, S., Troiani, H.E., de Iorio, A.R.F., 2023. Copper, zinc, and chromium accumulation in aquatic macrophytes from a highly polluted river of Argentina. Environ Sci Pollut Res 30, 31242–31255. https://doi.org/10.1007/s11356-022-24380-z.

[20] Hamidian, A.H., Jafari Ozumchelouei, E., Atashgahi, M., 2024. Assessment of Metal Pollution in Sediments and Their Bioaccumulation in *Phragmites australis* from Shoor River, Iran. Soil Sediment Contam 34, 1316–1343. https://doi.org/10.1080/15320383.2024.2420182.

[21] Skorbiłowicz, E., Skorbiłowicz, M., Sidoruk, M., 2024. The Bioaccumulation of Potentially Toxic Elements in the Organs of *Phragmites australis* and Their Application as Indicators of Pollution (Bug River, Poland). Water 16, 3294. https://doi.org/10.3390/W16223294.

[22] Alvarenga, P., Guerreiro, N., Simões, I., Imaginário, M.J., Palma, P., 2021. Assessment of the Environmental Impact of Acid Mine Drainage on Surface Water, Stream Sediments, and Macrophytes Using a Battery of Chemical and Ecotoxicological Indicators, 2021 Water 13, 1436. https://doi.org/10.3390/W13101436.

[23] Pérez-de-Mora, A., de Wilde, H., Paulus, D., Roosa, S., Onderwater, R., Paint, Y., Avignone Rossa, C., Farkas, D., 2024. Biostimulation of sulfate reduction for in-situ metal(loid) precipitation at an industrial site in Flanders, Belgium. Sci Total Environ 929, 172298. https://doi.org/10.1016/J.SCITOTENV.2024.172298.

[24] Lichtenthaler, H.K., 1987. [34] Chlorophylls and carotenoids: Pigments of photosynthetic biomembranes. Methods Enzym 148, 350–382. https://doi.org/10.1016/0076-6879(87)48036-1.

[25] Shrivastava, P., Khongphakdi, P., Palamanit, A., Kumar, A., Tekasakul, P., 2021. Investigation of physicochemical properties of oil palm biomass for evaluating potential of biofuels production via pyrolysis processes. Biomass– Convers Biorefin 11, 1987–2001. https://doi.org/10.1007/s13399-019-00596-x.

[26] Ardila, Y.C., Figueroa, J.E.J., Maciel, M.R.W., 2024. Mathematical models for predicting the higher heating value and ultimate analysis of biomass. Ind Crops Prod 208, 117777. https://doi.org/10.1016/J.INDCROP.2023.117777.

[27] Huang, Y.F., Lo, S.L., 2020. Predicting heating value of lignocellulosic biomass based on elemental analysis. Energy 191, 116501. https://doi.org/10.1016/j.energy.2019.116501.

[28] Curiel-Alegre, S., Khan, A.H.A., Rad, C., Velasco-Arroyo, B., Rumbo, C., Rivilla, R., Durán, D., Redondo-Nieto, M., Borràs, E., Molognoni, D., Martín-Castellote, S., 2025. Bioaugmentation and vermicompost facilitated the hydrocarbon bioremediation: scaling up from lab to field for petroleum-contaminated soils. Environ Sci Pollut Res 32, 16601–16616. https://doi.org/10.1007/s11356-024-32916-8.

[29] Silveira, M.L., Alleoni, L.R.F., O'Connor, G.A., Chang, A.C., 2006. Heavy metal sequential extraction methods—A modification for tropical soils. Chemosphere 64, 1929–1938. https://doi.org/10.1016/J.CHEMOSPHERE.2006.01.018.

[30] Tessier, A., Campbell, P.G.C., Bisson, M., 2002. Sequential extraction procedure for the speciation of particulate trace metals. Anal Chem 51, 844–851. https://doi.org/10.1021/AC50043A017.

[31] Khan, A.H.A., Nawaz, I., Yousaf, S., Cheema, A.S., Iqbal, M., 2019. Soil amendments enhanced the growth of *Nicotiana alata* L. and *Petunia hydrida* L. by stabilizing heavy metals from wastewater. J Environ Manag 242, 46–55. https://doi.org/10.1016/j.jenvman.2019.04.040.

[32] Aftab, N., Saleem, K., Khan, A.H.A., Butt, T.A., Mirza, C.R., Hussain, J., Farooq, G., Tahir, A., Yousaf, S., Zafar, M.I., Nawaz, I., 2021. *Cosmos sulphureus* Cav. is more tolerant to lead than copper and chromium in hydroponics system. Int J Environ Sci Technol 18, 2325–2334. https://doi.org/10.1007/s13762-020-02981-w.

[33] Curiel-Alegre, S., de la Fuente-Vivas, D., Khan, A.H.A., García-Tojal, J., Velasco-Arroyo, B., Rumbo, C., Soja, G., Rad, C., Barros, R., 2024. Unveiling the capacity of bioaugmentation application, in comparison with biochar and rhamnolipid for TPHs degradation in aged hydrocarbons polluted soil. Environ Res 252, 118880. https://doi.org/10.1016/j.envres.2024.118880.

[34] Štampar, M., Breznik, B., Filipič, M., Žegura, B., 2020. Characterization of In Vitro 3D Cell Model Developed from Human Hepatocellular Carcinoma (HepG2) Cell Line. Cells 9, 2557. https://doi.org/10.3390/cells9122557.

[35] Fey, S.J., Wrzesinski, K., 2012. Determination of Drug Toxicity Using 3D Spheroids Constructed From an Immortal Human Hepatocyte Cell Line. Toxicol Sci 27, 403–411. https://doi.org/10.1093/toxsci/kfs122.

[36] Wrzesinski, K., Alnøe, S., Jochumsen, H.H., Mikkelsen, K., Bryld, T.D., Vistisen, J. S., Willems Alnøe, P., Fey, S.J., 2021. A Purpose-Built System for Culturing Cells as In Vivo Mimetic 3D Structures. In: Haider, Z.S., Abdurakhmonov, I.Y., Barkaoui, A. (Eds.), Biomechanics and Functional Tissue Engineering. IntechOpen, pp. 1–21. https://doi.org/10.5772/intechopen.96091.

[37] Song, B., Xue, Y., Yu, Z., He, Y., Liu, Z., Fang, J., Wang, Y., Adams, J.M., Hu, Y., Razavi, B.S., 2024. Toxic metal contamination effects mediated by hotspot intensity of soil enzymes and microbial community structure. J Hazard Mater 466, 133556. https://doi.org/10.1016/J.JHAZMAT.2024.133556.

[38] Zandalinas, S.I., Peláez-Vico, M.Á., Sinha, R., Pascual, L.S., Mittler, R., 2024. The impact of multifactorial stress combination on plants, crops, and ecosystems: how should we prepare for what comes next? Plant J 117, 1800–1814. https://doi.org/10.1111/TPJ.16557.

[39] Khan, A.H.A., Kazmi, S.Z., Mirza, C.R., Butt, T.A., Gul, N., Barros, R., Yousaf, S., Iqbal, M., 2023. Effect of Soil Amendments on the Enzymatic Profile of Soil when *Nicotiana alata* L. and *Petunia hybrida* L. were Irrigated with Synthetic Heavy Metal-contaminated Wastewater. Chiang Mai J Sci 50, e2023008. https://doi.org/10.12982/CMJS.2023.008.

[40] Aponte, H., Meli, P., Butler, B., Paolini, J., Matus, F., Merino, C., Cornejo, P., Kuzyakov, Y., 2020. Meta-analysis of heavy metal effects on soil enzyme activities. Sci Total Environ 737, 139744. https://doi.org/10.1016/J.SCITOTENV.2020.139744.

[41] Sakin, E., Yanardağ, H., Ramazanoğlu, E., Yalçın, H., Yanarda, I.H., Ramazano Glu, E., Yalc ın, H., 2024. Enzyme activities and heavy metal interactions in calcareous soils under different land uses. Int J Phytoremediat 26, 273–286. https://doi.org/10.1080/15226514.2023.2238818.

[42] Zhang, Y., Li, T., Fu, Q., Hou, R., Li, M., Liu, D., Shi, G., Yang, X., Xue, P., 2024. Drip irrigation reduces the toxicity of heavy metals to soybean: By moving heavy metals out of the root zone and improving physiological metabolism. Agric Water Manag 292, 108670. https://doi.org/10.1016/J.AGWAT.2024.108670.

[43] Kanza Saleem, Zaman, A., Butt, T.A., Mirza, C.R., Iqbal, A., Khan, A.H.A., Yousaf, S., Iqbal, M., 2023. Uptake and Distribution of Cadmium and Copper by *Solanum lycopersicum* L. and Changes in the Metabolite Production. Biol Bull 50, 390–399. https://doi.org/10.1134/S1062359022602245.

[44] Qurban, M., Mirza, C.R., Khan, A.H.A., Khalifa, W., Boukendakdji, M., Achour, B., Yousaf, S., Nawaz, I., Butt, T.A., Iqbal, M., 2021. Metal Accumulation Profile of Catharanthus roseus (L.) G.Don and Celosia argentea L. with EDTA Co-Application, 2021, Vol. 9, Page 598 Processes 9, 598. https://doi.org/10.3390/PR9040598.

[45] Van Vuuren, J., M., Schoeman, Y., Botha, A.-M., Oberholster, P.J., 2024. Revealing the Protective Dynamics of an Ecologically Engineered Wetland against Acid Mine Drainage: A Case Study in South Africa. Appl Sci 14, 7441. https://doi.org/10.3390/APP14177441.

[46] Maranho, L.T., Gomes, M.P., 2024. Morphophysiological Adaptations of Aquatic Macrophytes in Wetland-Based Sewage Treatment Systems: Strategies for Resilience and Efficiency under Environmental Stress. Plants 13, 2870. https://doi.org/10.3390/PLANTS13202870.

[47] Khan, A.H.A., Soto-Cañas, A., Rad, C., Curiel-Alegre, S., Rumbo, C., Velasco-Arroyo, B., de Wilde, H., Pérez-de-Mora, A., Martel-Martín, S., Barros, R., 2025. Macrophyte assisted phytoremediation and toxicological profiling of metal(loid)s polluted water is influenced by hydraulic retention time. Environ Sci Pollut Res 32, 16760–16779. https://doi.org/10.1007/S11356-024-33934-2.

[48] Sharma, N., Wang, Z., Catalano, J.G., Giammar, D.E., 2022. Dynamic Responses of Trace Metal Bioaccessibility to Fluctuating Redox Conditions in Wetland Soils and Stream Sediments. ACS Earth Space Chem 6, 1331–1344. https://doi.org/10.1021/ACSEARTHSPACECHEM.2C00031.

[49] Ayaz, M., Khan, A.H.A., Song, K., Ali, A., Yousaf, S., Kazmi, A., Rashid, A., 2025. Integration of physio-biological methods for remediation of dyes and toxic metals from textile wastewater. Bioresour Technol Rep 29, 102044. https://doi.org/10.1016/J.BITEB.2025.102044.

[50] Alshehri, K., Gao, Z., Harbottle, M., Sapsford, D., Cleall, P., 2023. Life cycle assessment and cost-benefit analysis of nature-based solutions for contaminated land remediation: A mini-review, 2405–8440 Heliyon 9. https://doi.org/10.1016/J.HELIYON.2023.E20632.

[51] Guidi Nissim, W., Castiglione, S., Guarino, F., Pastore, M.C., Labra, M., 2023. Beyond Cleansing: Ecosystem Services Related to Phytoremediation. Plants 12, 1031. https://doi.org/10.3390/PLANTS12051031.

[52] Vargas-Moreno, J.M., Callejón-Ferre, A.J., Pérez-Alonso, J., Velázquez-Martí, B., 2012. A review of the mathematical models for predicting the heating value of biomass materials. Renew Sustain Energy Rev 16, 3065–3083. https://doi.org/10.1016/J.RSER.2012.02.054.